Journal of the European Ceramic Society 22 (2002) 1513–1524

www.elsevier.com/locate/jeurceramsoc

Sintering behaviour of composite materials borosilicate glass-ZrO_2 fibre composite materials

M.J. Pascual, A. Durán*, L. Pascual

Instituto de Cerámica y Vidrio (CSIC), 28500 Arganda del Rey, Madrid, Spain

Received 28 February 2001; received in revised form 4 October 2001; accepted 13 October 2001

Abstract

The characteristics and properties of mixtures of a borosilicate glass and ZrO_2 fibres obtained from compacts isothermally sintered are presented. Three different particle sizes of glass powder and different sintering temperatures and times have been used to reveal the influence of the specific surface area and the glass matrix viscosity on sintering. The fundamental developed aspects are the sintering kinetics, the dense material characterisation and the study of the sintering mechanisms. The composite materials are suitable for sealing molten carbonate fuel cells (MCFC). © 2002 Elsevier Science Ltd. All rights reserved.

Keywords: Borosilicate glass; Composites; Fibres; Fuel cells; Glass; Sintering; ZrO_2-fibres

1. Introduction

Composite materials of vitreous matrix loaded with ceramics (ceramic-filled-glass, CFG) are more and more used in different applications since they provide the necessary flexibility to design and develop new materials with a suitable combination of electrical, thermal and mechanical properties for specific applications.[1,2] Although the process facility at low temperatures is the greatest advantage of CFG composite materials, sintering reproducibility and high densification (that is, $\rho >$ 95% of theoretical density) is often a problem. In order to get acceptable reliabilities in mechanical behaviour, it is necessary to understand and control the densification of CFG and the development of the microstructure during sintering.

CFG composite materials with low sintering temperature density by a combination of glass redistribution, grain rearrangement and viscous flow in a three stage process described as "non-reactive liquid phase sintering " (NLPS).[1,2] The porous size, the ceramic particles characteristics, their concentration and a combination of glass properties such as viscosity, wetability, surface tension and particle size control the densification during NLPS.[1,3] The final stage of this process determines the microstructure and properties of the composite material.

The densification kinetics during NLPS has been modelled using the liquid phase non-reactive theory modified by the viscous sintering. During the final stage, densification of the composite material depends on the surface tension of glass and the viscosity of the CFG. The sintering time increases with the increase of viscosity that also increase with the filler concentration and/or the glass viscosity.

The glass viscosity has the most pronounced effect on the maximum filler concentration and the densification of the composite material, and it is the critical property that must be controlled when composite materials are designed and processed. With a high viscosity and low filler concentration good final densification can be obtained, but to produce high density composite materials with a high filler concentration, lower viscosity glasses must be used.

Jean and Gupta[4–6] used the NLPS model to describe the sintering behaviour of the borosilicate–cordierite glass system, as well as ceramic loaded with borosilicate glass.[7]

The presence of rigid inclusions in a glass powder compact provides different sintering rates generating stresses during sintering.[8] These stresses not only delay the densification rate of the compacts but also they can produce defects such as cracks generation.[9,10] Some

* Corresponding author.
E-mail address: aduran@icv.csic.es (A. Durán).

PII: S0955-2219(01)00479-4

authors[8–11] have tried to analytically determine the developed stresses during sintering and their effect on densification. Scherer[12] modelled the effect of rigid inclusions that is, non-sintering uncompressible inclusions, on sintering and applied the theory to the case of viscous sintering. Two models were considered. In the first one, the composite material was represented as one sphere composed by a central inclusion surrounded by the sintering matrix. This model has been employed by other authors to treat the same problem and it can be applied to low volume fractions of inclusions where the fields of inclusions tensions are not overlapped. The second model is related to a compact constituted by bimodal particle size distribution.[13] This model, called a "self-consistent model", can be applied up to the point where the inclusion volume fraction is so great that a continuous network can be formed that suppresses the contraction of the composite material. For the case of viscous sintering, the predictions of both models are undistinguished for volume fraction of inclusions lower than 0.2. Subsequently, Scherer used the self-consistent model for the viscous sintering of a material with a porosity of arbitrary distribution in presence of rigid inclusions.[14]

Rahaman and colleagues[15] carried out an experimental study on the densification of soda-lime glass compacts containing different volume fractions of silicon carbide particles. The authors found good agreement between the densification rates and those predicted by the rule of mixtures for silicon carbide volume fractions $\leqslant 0.1$. The data for the densification rates and the stresses caused by the inclusions are in excellent agreement with the Scherer theory for volume fractions $\leqslant 0.12$. These results suggest that it is possible to obtain composite materials of high density by means of conventional sintering (without pressure) for volume fractions $\leqslant 0.15$ by a viscous flow mechanism. Dutton and Rahaman[16] studied the sintering, creep and electrical conductivity of model composite materials of vitreous matrix as a function of the content and size of inclusions. The composite materials were formed by spherical particles of soda-lime glass and spherical nickel inclusions. They did not observe any effect of the inclusion size on viscosity at volume fractions below 10%. Above this value, it exists an effect of the inclusion size with an important increase of viscosity due to the interactions between inclusions. The sintering rates were compared with the predictions of the Scherer self-consistent model and the authors found good agreement when substituting the creep viscosity values in the model equation.

Boccaccini[17] studied the effect of the addition of Al_2O_3 platelets on the densification without pressure of a conventional aluminosilicate glass by heating microscopy. The creep rates and the hydrostatic stresses calculated by the Scherer model were in good agreement with the experimental results.

In the Raj and Bordia approximation[9] to the problem of inhomogeneous sintering, the deformation flow and the densification are described with simple expressions. These authors obtained solutions for the medium contraction rate and the interfacial tension in the composite material.

In this work, the sintering behaviour of mixtures of a borosilicate glass and ZrO_2 fibres has been studied as a function of the particle size of the glass powder, sintering temperature and time. The experimental results are explained by using different sintering models for a glass matrix containing rigid inclusions. The aim was to increase the corrosion resistance of the base glass against molten carbonates without changing much the thermal properties, that makes it adequate for sealing molten carbonate fuel cells (MCFC).[18,19]

2. Experimental procedure

A borosilicate glass with composition $60SiO_2{\cdot}24B_2O_3{\cdot}16Na_2O$, mol% (SiBNa403) has been used for this study. The batch was prepared from silica sand, reagent grade Na_2CO_3 and vitreous B_2O_3, and melted in air in a Pt crucible in a electric furnace at 1500 °C for 1 h.

After melting, the glass was milled and sieved to obtain three different particle sizes, fraction A, B and C. The particle size distributions corresponding to these powder fractions were determined by the laser scattering method with an equipment Mastersizer S, Malver Instruments Ltd. The specific surface area was measured by BET employing a Monosorb Surface Area Analyser MS-13 of Quantachrome. The glass powder morphology was observed by scanning electron microscopy (SEM), with a Zeiss-DSM 950 microscope.

A commercial zirconia fibre stabilised with yttria (8% weight) with 1.6 mm of medium length and 3–6 μm of diameter was employed for the preparation of the composite material.

Borosilicate glass powders with different particle sizes were mixed with the zirconia fibres in different proportions with the help of acetone employing a Turbula Mixer (System Schatz) from WAB for 2 h. The fibres and the glass powder were previously introduced in ultrasound to avoid the formulation of aglomerates.

Cylindrical samples ($\approx$1 cm height and $\approx$0.8 cm diameter) were prepared from the different mixtures by isostatic pressing at 200 MPa for 1 min. The samples were weighed and their dimensions measured.

The compacts were isothermally treated in electrical furnace in air at temperatures between 600 and 750 °C during different times. The densities of the green and treated samples were measured by Archimedes method employing Hg. The sintering process was followed from the density variations and the dimensional modifications of the samples.

For the composite material glass-zirconia, the theoretical density was calculated from the rule of mixtures (1):

$$\rho_{th} = \sum V_i \rho_i \quad (1)$$

where ρ_{th} is the theoretical sample density, V_i the volume fraction of phase i, and ρ_i its theoretical density.

The microstructure of the treated samples was observed by SEM. The treated samples were studied by X ray diffraction (XRD) to detect the presence of possible crystallisation in the vitreous matrix using a Siemens model D5000 diffractometer with Kristalloflex 710 equipment.

The viscosity-temperature curve of the glass has been determined by the rotation method, for viscosities in the range 10–10^5 dPa s, and the fibre elongation method, for viscosities in the range 10^8–10^{13} dPa s. The measurements were performed with a Haake high temperature viscometer that allows the combination of both methods using a Sensor System HE 1700. The employed method are described in the ISO 7884-2[20] and ISO 7884-3 standards.[21]

The viscosity (η) data obtained using both methods were adjusted to the Vogel–Fulcher–Tamman, VFT, Eq. (2) employing a regressive calculation with all viscosity experimental points in the studied range. From this fit, the values of the constants of the viscosity equation A, B and T_0 were obtained:

$$\log\eta = A + \frac{B}{T - T_0} \quad (2)$$

3. Results and discussion

3.1. Viscosity of the glass matrix

Fig. 1 represents the viscosity of SiBNa403 glass as a function of temperature. The experimental points are situated in two viscosity ranges, $\log\eta > 8$ and $\log\eta < 4$, with η in dPa s, both corresponding to the acquired data through the techniques employed in the viscosity measurement: the fibre elongation method and the rotation method. The viscosity values for each glass have been fitted to the VFT equation [Eq. (2)], the continuous line in Fig. 1 being calculated from these values.

The figure allows to determine the viscosity values of the glasses in the working temperature range of the cell (650–750 °C), relevant for the application envisaged for this glass. SiBNa403 presents adequate viscosity values for its application in MCFC since at 650 °C $\log\eta = 8$ and at 750 °C viscosity is not lower than $\log\eta = 5.5$. These viscosity values are low enough to allow sealing but high enough to avoid flowing. These conditions are necessary to reach good chemical resistance and to lower the molten carbonates attack as well as to enhance mechanical resistance against compression.[22]

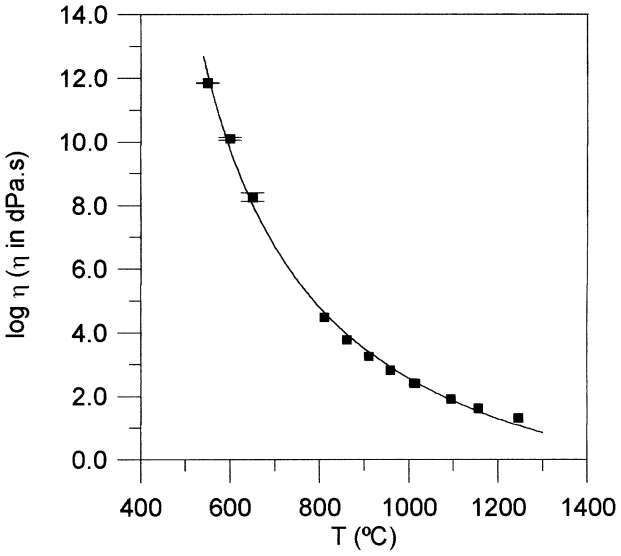

Fig. 1. Viscosity-temperature curve for SiBNa403 glass.

3.2. Sintering kinetics

Table 1 shows the mean particle sizes and specific surface area of the glass powders used. Fraction A (20–40 μm) of SiBNa403 glass presents a monomodal size distribution with a medium particle size diameter, d_{50}, around 35.9 μm. Fraction B shows a multimodal distribution extended between 40 and 50 μm and ≈1 μm and fraction C exhibits also multimodal distribution between 10 and 20 μm and ≈1 μm.

The theoretical density of the composite material was calculated from the densities of SiBNa403 glass (2.46 g cm^{-3}) and cubic zirconia (6.09 g cm^{-3}) employing the rule of mixtures [Eq. (1)]. The fibre volume fractions employed were F= 0.09 (9 vol.%, 20 wt.%), F=0.21 (21 vol.%, 40 wt.%), F= 0.38 (38 vol.%, 60 wt.%) and F 0.62 (62 vol.%, 80 wt.%). For example, for a volume fraction of ZrO_2 F=0.09 the theoretical density results 2.79 g cm^{-3}. Fig. 2 represents the relative density, ρ, as a function of sintering time at 625 °C for the powder glass corresponding to the smallest particle size, fraction C, and containing different volume fractions of ZrO_2 fibres, F. The sintering behaviour without fibre (F=0) has been also represented for the same particle size

Table 1
Specific surface area and mean particle size of SiBNa403 glass powders

Fraction	d_{50} (μm)	Specific surface area (m^2/g)
A (40–20 μm)	35.9±0.5	0.19±0.05
B (<20 μm)	10.9±0.5	0.72±0.05
C (<20 (μm)	6.3±0.5	1.90±0.05

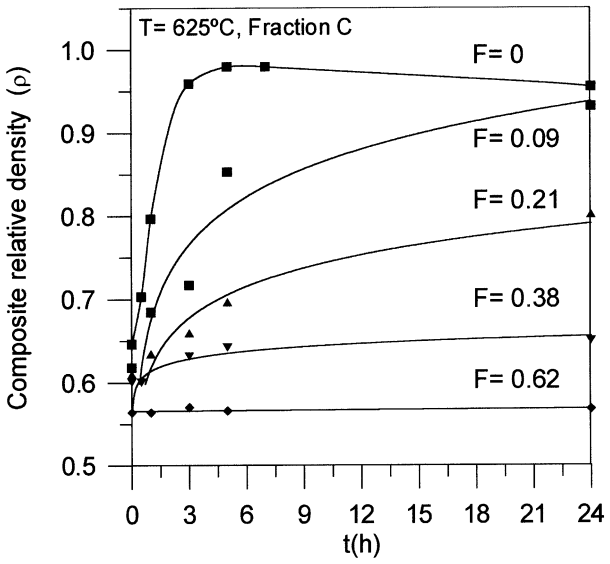

Fig. 2. Relative density of the composite material SiBNa403 glass/ZrO_2 fiber versus sintering time for fraction C of powder glass and different volume fractions, F, at 625 °C.

distribution. The viscosity of the glass at this temperature is equal to 1.4×10^9 dpa s ($\log\eta=9.15$) (Fig. 1). The glass sintered up to 98% of theoretical density after 5 h while the maximum densification reached for composites was 0.94 after 24 h of treatment with a volume fraction equal to 0.09. The smaller the fibre content the greater was the densification degree.

Thus, it seems evident that to obtain densities higher than 80% at temperatures in this range, the maximum fibre fraction should be $F\sim 0.09$. Thus, the densification study of the mixtures at different temperatures and particle sizes will be carried out on samples with this fibre percentage.

Fig. 3a, b and c presents the sintering behaviour of mixtures of SiBNa403 glass with 9 vol.% ZrO_2 fibres ($F=0.09$) treated at 650 °C for the three particle sizes compared with the sintering of the corresponding glass ($F=0$).

The viscosity of the glass matrix at this temperature is $\log\eta=8.3$. The maximum relative density for SiBNa403 glass ($\rho=0.98$) is reached after 5 h of treatment with powder of fraction A while the same sintering is reached with fraction B after 3 h and only after 0.5 h for fraction C. Once the maximum density is reached, longer treatment times lead to a diminution of the density for all the particle size distributions.

A maximum density of 0.94 is reached after 3 h at 650 °C for the mixture of the ZrO_2 fibre with the powder glass with the smaller particle size (fraction C) (Fig. 3c). When greater particle sizes are employed, around 5 h are necessary to reach a maximum relative density $\rho=0.84$, indicating that the increase of the matrix particle size along with the presence of ZrO_2 inhibit a major densification.

Fig. 4 compares the sintering behaviour of the samples with the smallest particle size (fraction C) treated at 625 and 650 °C showing the important effect of viscosity on the densification rate. When fraction C is employed, sintering times of 24 h are necessary to obtain a relative density equal to 0.94 at 625 °C ($\log\eta=9.5$) while the same densification is reached after three hours at 650 °C ($\log\eta=8.3$).

The XRD pattern of samples treated at 650 °C during 24 h showed α-quartz and ZrO_2 with the same crystallographic structure than initial fibres (Fig. 5). α-quartz has been also detected for long treatments at 625 °C.

Fig. 6a is a microphotograph of a compact of the mixture with fraction C sintered for 3 h at 650 °C ($\rho=0.94$). In these conditions, the composite has reached the maximum densification level and most part of the porosity is concentrated around the ZrO_2 fibres. This porosity could be related to stresses present in the interface glass/fibre during sintering. Fig. 6b shows the microstructure of a sample treated at 650 °C during 24 h and

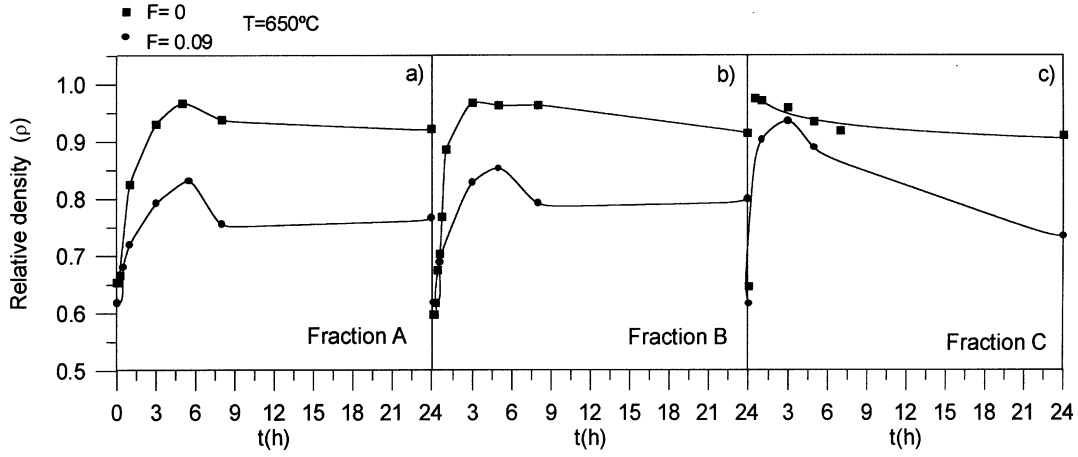

Fig. 3. Relative density of SiBNa403 glass ($F=0$) and of the composite material ($F=0.09$) versus sintering time for different particle size of powder glass at 650 °C.

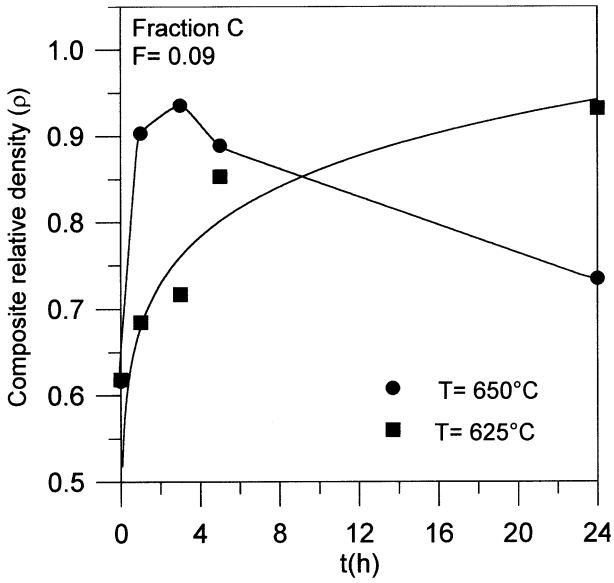

Fig. 4. Relative density of the composite material ($F=0.09$) versus sintering time for powder glass fraction C, $T=625$ and 650 °C.

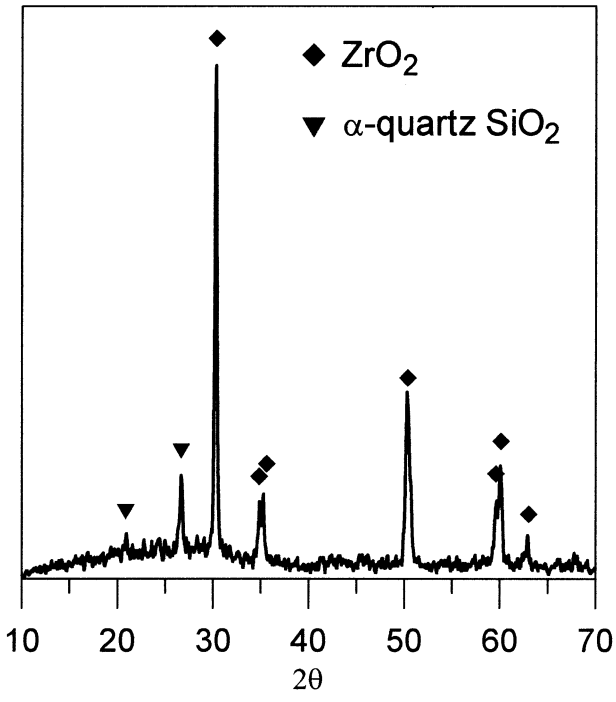

Fig. 5. Diffractogram corresponding to the mixture treated at 650 °C for 24 h. $F=$ 0.09, fraction C.

with a relative density of 0.75. New porosity originated around the quartz crystals developed during the long time thermal treatment.

The density of α-quartz (2.65 g cm^{-3}) is greater than the density of the glass (2.46 g cm^{-3}), but crystallisation implicates a volume decrease of 15% producing the opening of porosity and decreasing the relative density. The α-quartz crystallisation is expected because of the location of the glass composition in the phase diagram

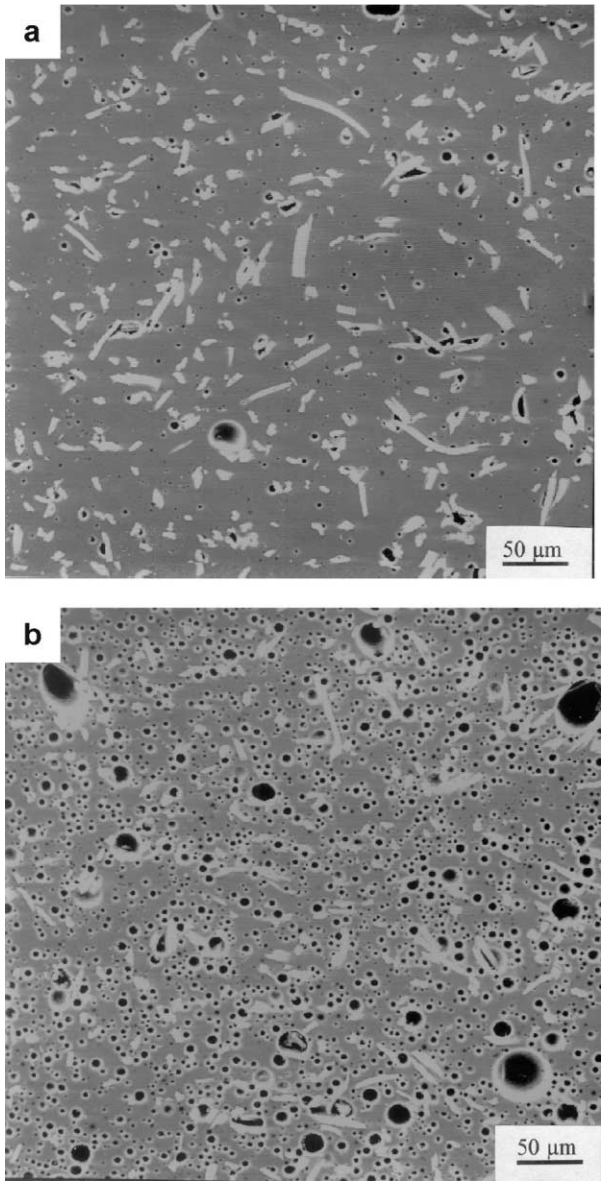

Fig. 6. Microstructure of the mixture $F=0.09$, fraction C, treated at 650 °C for (a) 3 h ($\rho=$ 0.94) and (b) 24 h ($\rho=0.75$).

of the system Na_2O–B_2O_3–SiO_2.[23] On the other hand, the crystallisation process can be accompanied by gas release that would also produce a density decrease [24].

Fig. 7a is microphotograph corresponding to a sample of fraction A with a 9 vol.% of ZrO_2 fibre densified at 650 °C for 5 h ($\rho=0.85$), showing some porosity around the fibres. The microphotograph shows that the morphology of the fibres maintains after thermal treatment indicating a rather slight dissolution of zirconia into the glass matrix.

The extension of zirconia dissolution has been determined by microanalysis EDS making a Zr mapping, Fig. 7b, that shows a quite uniform distribution of Zr dissolved into the glass matrix.

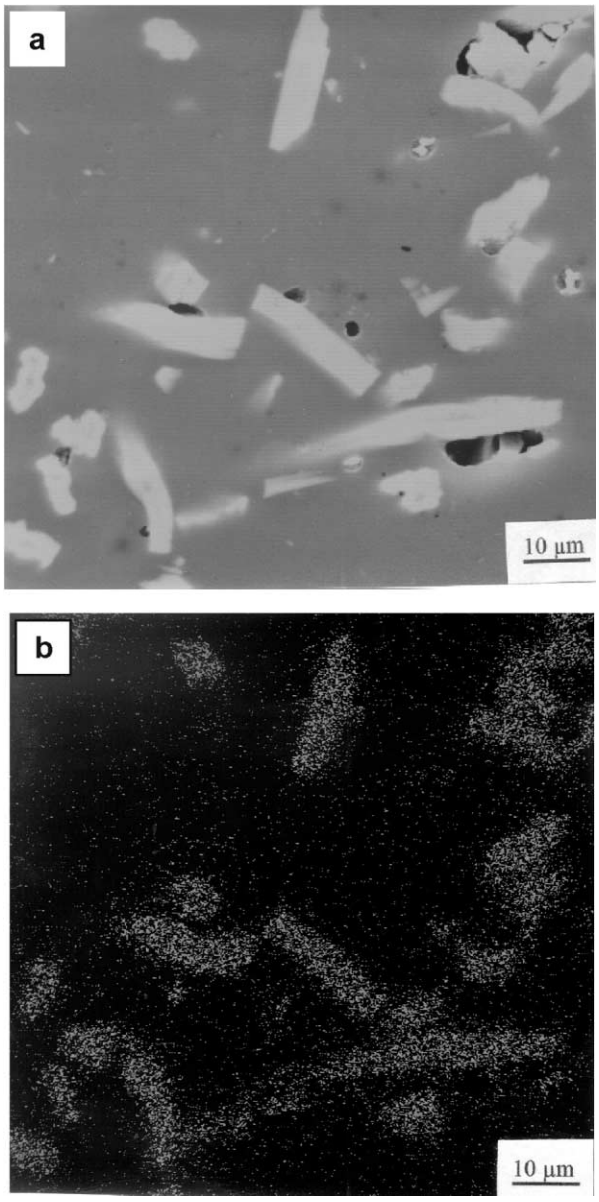

Fig. 7. (a) Microstructure of the mixture $F=0.09$, fraction B, treated at 650 °C for 5 h ($\rho=0.85$), (b) microanalysis of Zr of the same sample.

The dissolution of Zr in the glass matrix should not much influence the density but it can be an important factor on viscosity, thermal expansion and chemical resistance of the glass, and thus has to be taken into account when studying the properties of the composite materials.

The densification rate of the composite material can be obtained from the densification data as a function of time fit to a polinomic function followed by differentiating and application of the equation:

$$\overset{0}{\varepsilon}_{\rho} = \frac{\overset{0}{\rho}}{\rho} \tag{3}$$

where $\overset{0}{\varepsilon}_{\rho}$ is the densification rate,
$\overset{0}{\rho}$ the derivate of the densification curve and
ρ the relative density

In Fig. 8a, the densification rates of the glass and the composite material with 9% vol. fibre can be observed for two different particle sizes. The greater particle sizes (fractions A and B) lead to relative densities not higher than 0.85 at 650 °C and lower than 0.8 at 625 °C even for sintering times up to 24 h. The similar behaviour of the curves could be explained through the same sintering mechanism in which the greater the particle size and the higher the fibre fraction the lower is the sintering rate. Fig. 8b shows the strong effect of the glass viscosity on the densification rate, that increases around one order of magnitude when viscosity changes from $\log\eta=9.15$ to $\log\eta=8.3$.

Thus, the control of viscosity, particle size of the glass powder and sintering time may allow sintering composites with the same ratio glass/fibre at different velocities. If low sintering temperatures are required, it is possible to work at viscosities of the glass matrix as high as $\log\eta=9.15$ decreasing the particle size of the glass and increasing the sintering time.

3.3. Thermal properties

The thermal properties of some of the prepared glass/zirconia composite materials have been studied to evaluate the changes produced by ZrO_2 addition in the transformation temperature, T_g, dilatometric softening temperature, T_d, as well as in the thermal expansion coefficient, α. Table 2 shows the values for T_g, T_d and α of composites with $F=$ 0.09 and fraction C along with the temperature and time of sintering for obtaining the maximum density, compared with data corresponding to the glass sintered without fibre.

Glass SiBNa403 (fraction C) presents a maximum densification of 98% after 5 h of thermal treatment at 625 °C, the resulting thermal expansion coefficient is close to that of the bulk glass.

SiBNa403 glass with a 9 vol.% ZrO_2 and treated at 625 °C for 24 h reaches a maximum density of 0.94. T_g is equal to that of the glass matrix in the error range but the thermal expansion coefficient increases up to $9.0.10^{-6}$ K^{-1}. The same densification is obtained for a treatment at 650 °C after 3 h, T_g does not change with respect to the bulk glass and the thermal expansion coefficient increases up to $8.6{\cdot}10^{-6}$ K^{-1}. These slight changes in the properties of the sintered materials are not only due to ZrO_2 addition but also to quartz crystallisation that takes places along with the densification process, and that is more accused where for longer treatment times. The decrease of SiO_2 content in the glass matrix could explain the higher α value. Thus, since α values depend on crystallisation of sintering glass, they also depend on temperature and time of sintering treatment as well as on particle size.

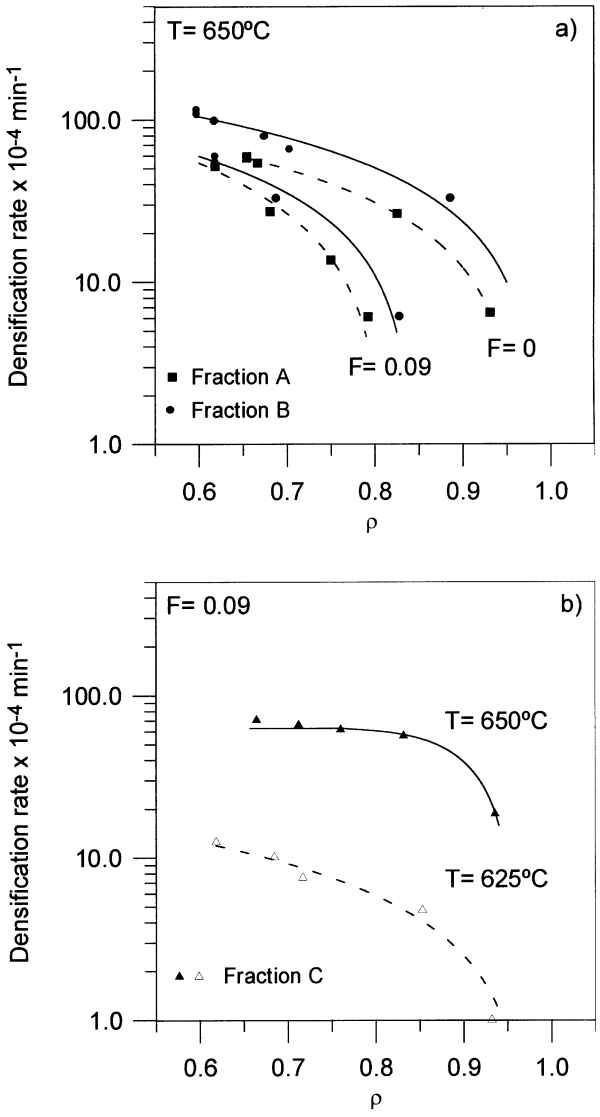

Fig. 8. Densification rate of the composite material versus relative density as a function of (a) the particle size and (b) sintering temperature.

3.4. Experimental results and theoretical models

The experimental data have been compared with the predictions of theoretical models related to the sintering of a matrix containing rigid inclusions, specially with the predictions of Scherer[12,14] and Raj and Bordia,[9] which are models that better describe the whole sintering process.

3.4.1. Scherer cylinder model for viscous sintering

The Scherer model for the glass sintering in absence of inclusions has been firstly applied.[25] Scherer proposed a simple model for the microstructure of a sintering compact consisting of a cubic arrangement formed by intersecting cylinders. The cylinders represent particles rows, and the radius corresponds to the average particle radius. Scherer calculated the sintering rate for this structure following the Frenkel theory and obtained a theoretical curve for the relative density versus the reduced time $K(t-t_0)$ where $K=\gamma n^{1/3}/\eta$, being n the number of porous per volume unit of real material, γ the superface tension and η the viscosity.

The reduced time, obtained from the theoretical curves of Scherer model, has been represented versus the sintering time in Fig. 9. The figure shows the behaviour of the glass of fractions B and C in absence ($F=0$) and in presence ($F=0.09$) of a secondary phase. The experimental data fit straight lines indicating a sintering mechanism by viscous flow.[26] The slope of the lines is related to the densification rates, decreasing when the particle size increases.

In the first densification steps, a particle rearrangement previous to the sintering by viscous flow can take place, this justifying the first points out of linearity. For intermediate treatment times, the data fit to a straight line according to a sintering mechanism by viscous flow. The experiment data abandon the linearity for long time as a consequence of devitrification processes already described.

3.4.2. Models for the sintering of a glass matrix containing rigid inclusions

3.4.2.1. Self-consistent Scherer model for the sintering with rigid inclusions. The self-consistent Scherer model,[14] derived for an isotopic, linearly viscous material have been also applied. Considering the effect of the stresses produced by the inclusions, Scherer demonstrated that the hydrostatic component of the tension field delays the matrix densification even more than predicted by the rule of mixtures. Thus, the relation between the real strain rate of the composite, $\dot{\varepsilon}_c$, and

Table 2
Thermal properties of the composite material (SiBNa403 glass/ZrO_2 fibre) (9 vol.%, fibre addition)

Material	Sintering treatment			T_g (°C)	T_R (°C)	$\alpha_{50-400\ °C}$ (K^{-1})×10^6
	T (°C)	t (h)	ρ			
SiBNa403 (bulk)	–	–	1	565±2	608±5	7.7±0.1
SiBNa403 (fraction C)	625	5	0.98	568±2	599±5	8.6±0.1
SiBNa403 (fraction C)+ZrO_2	625	24	0.94	562±2	611±5	9.0±0.1
SiBNa403 (fraction C)+ZrO_2	650	3	0.94	560±2	585±5	8.6±0.1

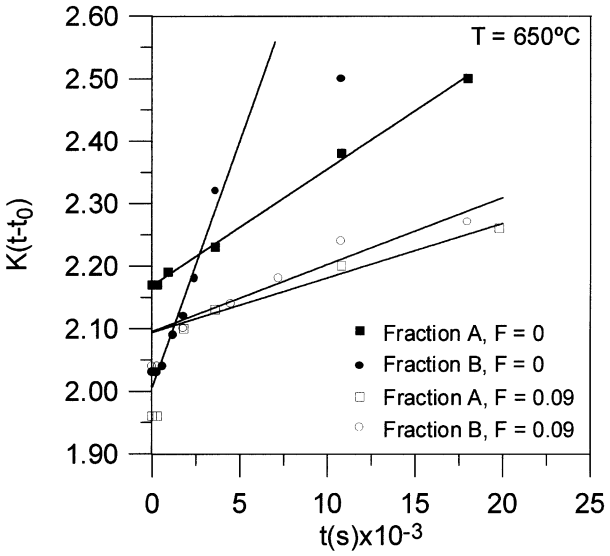

Fig. 9. Reduced time versus sintering time according to Scherer's model.[25].

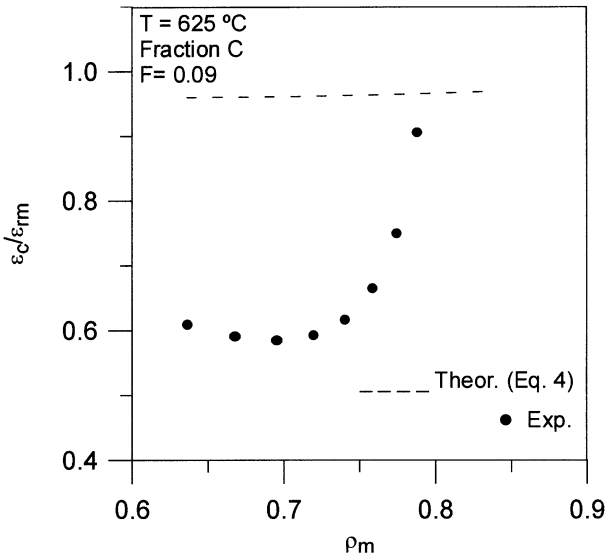

Fig. 10. Linear strain rate of the composite referred to the strain rate from the rule of mixtures versus relative density of the matrix for $F=0.09$, fraction C and $T=625\ ^{\circ}C$.

that predicted from the rule of mixtures, $\dot{\varepsilon}_{rm}$, can be expressed by

$$\frac{\dot{\varepsilon}_c}{\dot{\varepsilon}_{rm}} = \left\{1 + \frac{2\rho_m(1-A)}{(\rho_m + r)(1-0.5A)}\left[1 + \frac{7.5\rho_m(1-0.5A)}{r(4-2.5A)}\right]\right\}^{-1} \tag{4}$$

where $r=(1–F)/F$ and $A=[\rho_m/(3–2\rho_m)]^{1/2}$. Being F the volumetric fraction which corresponds to the fully dense composite and ρ_m the instantaneous absolute density of the glass matrix that can be expressed as

$$\rho_m = \frac{(\rho_{co} - \rho_i f_o)\rho_c}{(\rho_{co} - f_o\rho_c)} \tag{5}$$

where ρ_i is the density of the inclusion phase (fibres) and f_o is the volume fraction of fibres in the initial compact.

The instantaneous volume fraction of inclusions, f, the relative density of the matrix, ρ_m and F are related by the expression:[15]

$$f = \frac{\rho_m}{\rho_m + (1-F)/F} \tag{6}$$

Fig. 10 shows the theoretical values predicted by Scherer model and the experimental values obtained from Eq. (4) for $F=0.09$, fraction C and a treatment temperature of 625 °C. We considered only this case since the applicability of the model is limited to $F \leqslant 0.15$.[14,17] The deviation of the experimental data from the theoretical predictions is quite important in the first densification stage up to approximately $\rho=0.75$. This means that the effect of the tensions caused by the inclusions on the densification rate in the first densification stages is much greater than that predicted by the Scherer model, the sintering behaviour deviating considerably from the prediction of the rule of mixtures. During this stage, rearrangement processes of the glass powders and inclusions are responsible for the densification values. For $\rho>0.75$, the values approximate to that of the model suggesting that the stresses produced at the beginning of sintering tends to relax by viscous flow of the glass matrix. From this densification value, rearrangement processes are not so relevant and the viscous flow becomes the determining factor of the final densification of the composite material.

On the other hand, poor packing of glass particles around the fibres and the stress concentration in the interfaces glass/fibre could explain the presence of porosity around the fibres.

The deviation observed respect to the self-consistent Scherer model was expected since the geometry of the glass powder as well as the inclusions is assumed spherical in the model. Moreover it does not take into account the size of the inclusions.

Finally, these results and those obtained from the Scherer model in absence of rigid inclusions seem to agree with the sintering mechanism proposed by Ewsuk[1,2] for glasses filled with ceramics where the densification takes place by a combination of glass redistribution, grain rearrangement and viscous flow in a three stages process described *as non-reactive liquid phase sintering*.

3.4.2.2. Raj and Bordia model. Raj and Bordia[9] considered the simultaneity of the densification and the deformation or creep during the sintering process, con-

sidering of great importance the creep for the relaxation of the stress concentration due to an incompatible densification. The authors demonstrated that the effect of the inhomogeneities in the sintering behaviour of the composite material depends on the relationship between creep rate constant and densification rate constant. The theoretical results are simple for the special case of the sintering of a matrix containing inert particles of secondary phase. The densification as a function of time can be described as:

$$\frac{\Delta\rho}{\Delta\rho_{\max}} = 1 - \exp\left(\frac{-9\beta}{4F + 9\beta}\frac{t}{\tau}\right) \tag{7}$$

where $\Delta\rho$ is change in relative density for the composite material, $\Delta\rho_{\max}$ the change in relative density with respect to the maximum densification, β the ratio of the rate constant for creep, and the rate constant for densification, F the volume fraction of inclusions and τ the time to get the maximum densification.

The most relevant parameter of the analysis is β since it shows the possibility of tension relaxation by creep. If β is high ($\beta > 1$), the relaxation takes place and it is expected that the inclusions have a small or no effect on the matrix sintering. In these cases, the sintering behaviour should follow the rule of mixtures. On the other hand, if β is low ($\beta < 1$), the sintering velocity will be severely delayed and will deviate considerably from the rule of mixtures.[27,28]

The intrinsic behaviour of the matrix (without secondary phase) is expressed as:[9]

$$\left(\frac{\Delta\rho}{\Delta\rho_{\max}}\right)_{F=0} = 1 - \exp\left(-\frac{t}{\tau}\right) \tag{8}$$

From the plot $\ln[(1-\rho)/(1-\rho_0)]$ versus the sintering time, the value of τ was obtained for fraction C treated at 625 °C and fractions A and B treated at 650 °C.

In terms of τ, the parameter β can be estimated by means of the equation:[27,28]

$$\beta = \frac{3(1-2\nu)\tau P}{2(1+\nu)\eta \ln\left(\frac{1}{\rho_{fmo}}\right)} \tag{9}$$

where ρ_{fmo} is the initial relative density of the glass matrix free of inclusions, ν is the elastic Poisson ratio, P is the intrinsic sintering pressure and η is the viscosity of the glass matrix. Although ν also changes with density during sintering. The last two parameters are those that change more strongly with density during the sintering process. The variation of the sintering pressure with the density can be expressed in terms of the initial particle size of the glass powder matrix (r) as:[29]

$$P = \frac{2\gamma}{r}\left(\frac{\rho_{fm}}{1-\rho_{fm}}\right)^{1/3} \tag{10}$$

where γ is the surface tension of the glass and ρ_{fm} the instantaneous relative density of the glass matrix free of inclusions.

The effect of the density change on the glass viscosity of a porous glass has been studied theoretical and experimentally.[30] The following equation was derived

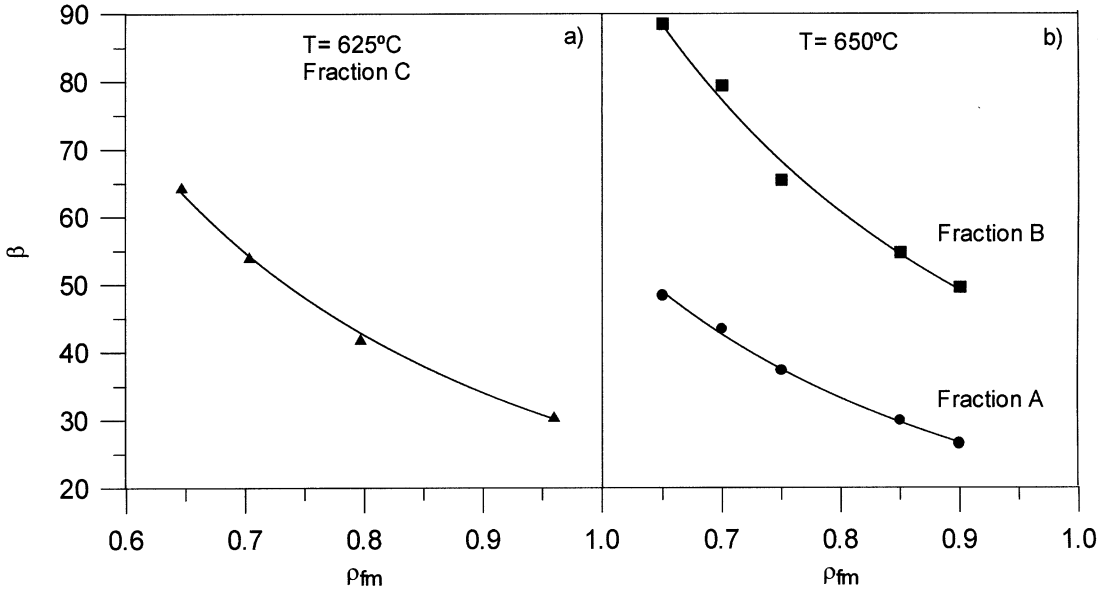

Fig. 11. β [see Eq. (9)] versus density of the glass matrix free of inclusions for (a) fraction C treated at 625 °C and (b) Fractions A and B treated at 650 °C.

from the analysis of elastic tensions using the viscous analogy:

$$\eta = \eta_0 \frac{3\Omega\rho_{fm}^2}{3\Omega\rho_{fm} + 2(1-\rho_{fm})} \quad (11)$$

where the shape factor, Ω, depends on the pore structure and varies between 0.15 and 0.20 for the low density range ($\rho_{fm} < 0.85$).

The β value [Eq. (9)], calculated from the glass properties, has been represented as a function of the density of the free matrix for fraction C treated at 625 °C and for fractions A and B treated at 650 °C (Fig. 11a, b). Eqs. (10) and (11) have been substituted in Eq. (9) with $\Omega = 0.15$ and it was established $\nu = 0.23$ and $\psi = 0.240$ N m^{-1}.[31] The used values of r, η_0 and τ are those of SiBNa403 glass. In all the cases, β calculated is greater than 1, so no deviation from the rule of mixtures is expected.

If the relationship $\ln[(\Delta\rho/\Delta\rho_{max})-1]$ versus the treatment time normalised by τ, t/τ [Eq. (7)] is plotted, β values can be also obtained for our actual sintering experiments with fibres.

Fig. 12a and b shows the dependence of β with the volume fraction of fibres and with the particle size. The values of β for the samples treated at 650 °C is one order of magnitude lower than that of those treated at 625 °C. The difference in viscosity between both temperatures is also of one order of magnitude log $\nu = 8.3$ at 650 °C and log η 9.15 at 625 °C. So, one order of magnitude in viscosity means one order of magnitude in the β value. The β values obtained directly from the experimental sintering results indicate, following the model, that glass flow is not enough to eliminate the tensions due to the differential densification caused by the presence of ZrO_2 fibres.

The strong deviation of experimental data from theoretical predictions show that the model does not fit the real sintering process.

Previous studies[15,17] presented a good agreement with the Scherer theory for sintering with rigid inclusions for volume fractions < 0.12, no dissolution of the inclusions into the glass matrix is considered in theses works. Nevertheless, neither the Scherer not the Raj and Bordia models give consistent fitting of experimental present data. None of both models take into account the size and geometry of the inclusions and their reactivity with the matrix. In our case, an important dissolution of the fibres into the matrix takes place during sintering and consequently there are changes in composition that cause an increase of viscosity and make the model not applicable.

However, the sintering process qualitatively agrees with the Scherer model in absence and presence of rigid inclusions, suggesting a mechanism in which the sintering takes place by a combination of glass redistribution, grain rearrangement and viscous flow in a three stages. Further work has to be done to approach theoretical models to more realistic situations.

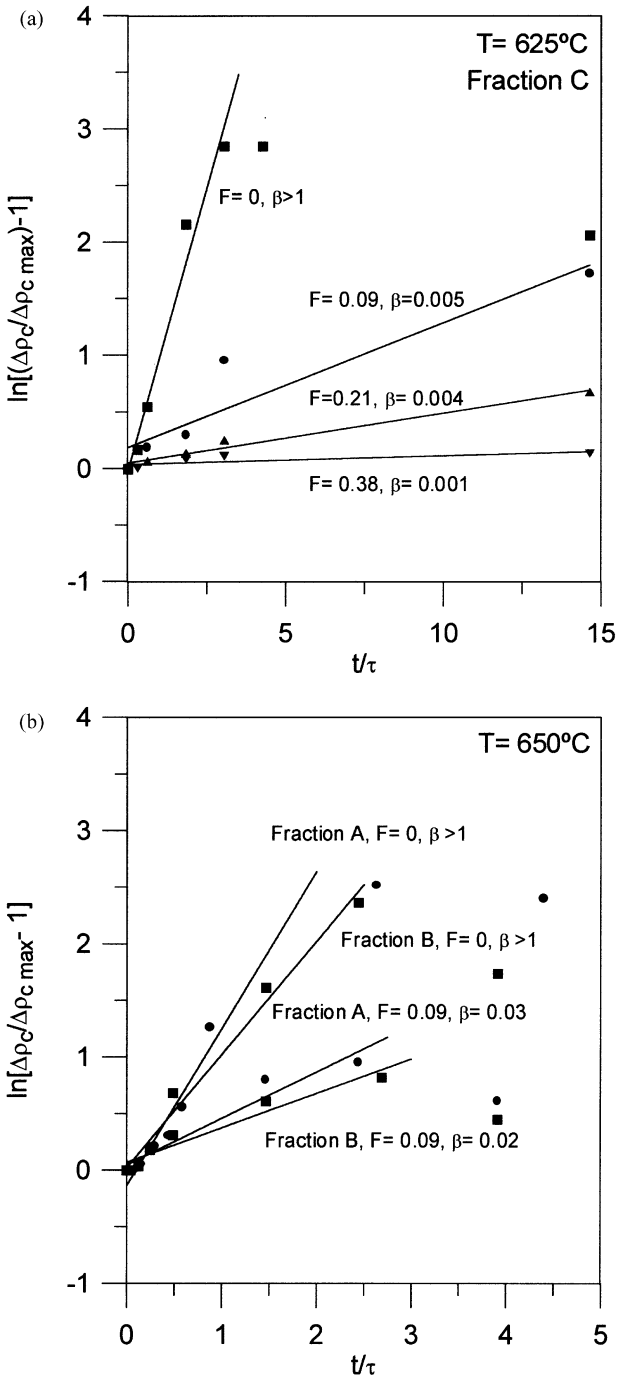

Fig. 12. β Values in presence of rigid inclusions. (a) fraction C, $T = 625$ °C, (b) Fractions B and C, $T = 650$ °C.

4. Conclusions

Borosilicate glass-zirconia fibre composite materials with adequate densification values and thermal properties

similar to that of the glass matrix have been prepared. The incorporation of zirconia allows to increase the corrosion resistance against molten carbonates as well as to obtain a better mechanical properties of the system thus constituting an improvement in the efficiency of the sealing material for the specific application in sealing MCFC.

Different particles sizes of the glass powder and different proportions glass/fibre have being used. The densification rate and the final density of the composites depend on the ratio of glass to fibre content with a maximum fibre content of 20 wt.% (9 vol.%) to obtain densities higher than 85%. For determined glass/fibre ratio, the selection of sintering temperature—and thus viscosity—the particle size of the glass and the sintering time allows to sinter at different rates, making possible to adapt the sealing to the specific requirements.

At the working temperature of the MCFC (650 °C), it is possible to sinter the composite material with a fibre volume fraction of 0.09 using the three studied powder particle sizes, but the fraction C ($d_{50} \approx 6$ μm) allows to sinter up to a densification greater than 0.94 in only 3 h. The great part of residual porosity in the samples concentrates around the ZrO_2 fibres, a possible consequence of the tensions in the interface glass/fibre during sintering and poor powder packing around the fibres.

After the maximum relative density is reached, longer treatment times cause quartz crystallisation from the glass matrix, that causes the diminution of the density by new porosity generation.

The sintering results do not fit the theoretical sintering models in presence of rigid inclusions, since these models do not consider the size and geometry of the inclusion as well as possible reactivity with the matrix. These facts together with the glass devitrification during sintering process make these models non-applicable to this case.

Acknowledgements

This work was funded by grants from the Joule project: ''Development of industrially relevant MCFC stacks'', Joule-CE (PL950478) and the research project MAT2000-0952-C02-01.

References

1. Ewsuk, K. G., Harrison, L. W. and Walczak, F. J., Sintering of glass-filled ceramic composites; effects of glass properties. In *Ceramic Powder Science, Part B*, ed. G. L. Messing, E. R. Fuller and H. Hausner. The American Ceramic Society, Westerville, OH, 1988, pp. 969–977.
2. Ewsuk, K. G., Ceramic-filled-glass composite sintering. *Ceram. Trans (Mater. Processes Microelectron. Syst.)*, 1990, **15**, 279–295.
3. Ewsuk, K. G., Effect of fillerloading on final-stage viscous sintering of ceramic-filled-glass composites. In *Ceramic Powder Processing Science*, ed. H. Hausner, G. L. Messing and S. Hirano. Deutsche Keramische Gesellschaft, Köln, FRG, 1989, pp. 747–754.
4. Jean, J.-H. and Gupta, T. K., Densification of the initial stage of liquid-phase sintering: glass-cordierite system. *J. Mater. Sci. Lett.*, 1992, **11**, 656–658.
5. Jean, J.-H. and Gupta, T. K., Liquid-phase sintering in the glass-cordierite system. *J. Mater. Sci.*, 1992, **27**, 1575–1584.
6. Jean, J.-H. and Gupta, T. K., Liquid-phase sintering in the glass-cordierite system: particle size effect. *J. Mater. Sci.*, 1992, **27**, 4967–4973.
7. Jean, Jau-Ho. and Gupta, T. K., Isothermal and nonisothermal sintering kinetics of glass-filled ceramics. *J. Mater. Res.*, 1992, **7**, 3342–3347.
8. Evans, A. G., Considerations of inhomogeneity effects in sintering. *J. Am. Ceram. Soc.*, 1982, **65**, 497–501.
9. Raj, R. and Bordia, R. K., Sintering behaviour of bimodal compacts. *Acta Metall.*, 1984, **32**, 1003–1019.
10. Hsueh, C. H., Evans, A. G., Cannon, R. M. and Brook, R. J., Viscoelastic stresses and sintering damage in heterogeneous powder compacts. *Acta Metall.*, 1986, **34**, 927–936.
11. Hsueh, C. H., Evans, A. G. and McMeeking, R. M., Influence of multiple heterogeneities on sintering rates. *J. Am. Ceram. Soc.*, 1986, **69**, C–64-C-66.
12. Scherer, G. W., Sintering with rigid inclusions. *J. Am. Ceram. Soc.*, 1987, **70**, 719–725.
13. Scherer, G. W., Viscous sintering of a bimodal pore size distribution. *J. Am. Ceram. Soc.*, 1987, **67**, 709–715.
14. Scherer, G. W., Viscous sintering with a pore-size distribution and rigid inclusions. *J Am. Ceram. Soc.*, 1988, **71**, C–447-C-448.
15. Rahaman, M. N. and De Longhe, L. C., Effect of rigid inclusions on the sintering of glass powder compacts. *J. Am. Ceram. Soc.*, 1987, **70**, C–348-C-351.
16. Dutton, R. E. and Rahaman, M. N., Sintering, creep, and electrical conductivity model glass-matrix composites. *J. Am. Ceram. Soc.*, 1992, **75**, 2146–2154.
17. Boccaccini, A. R., Sintering of glass matrix composites containing Al_2O_3 platelet inclusions. *J. Mater. Sci.*, 1994, **29**, 4273–4278.
18. Pascual, M. J., Durán, A. and Pascual, L. Viscosity and thermal properties in the system R_2O–B_2O_3–SiO_2, R = Li, K, Na. *Physics and Chemistry of Glasses*, in press.
19. Pascual, M. J., Durán, A. and Pascual, L. Sintering process of glasses in the system Na_2O-B_2O_3-SiO_2. *J Non-Cryst. Solids.*, in press.
20. *Glass-Viscosity and Viscometric Fixed Points—Part 2: Determination of Viscosity by Rotation Viscometers*. ISO 78 84-2 First edition 1987-12-15.
21. *Glass-Viscosity and Viscometric Fixed Points—Part 3: Determination of Viscosity by Fibre Elongation Viscometer*. ISO 7884-3 First edition 1987-12-14.
22. Pascual, M. J. *Vitreous Materials for Sealing Molten Carbonate Fuel Cells (MCFC)*. PhD thesis, Instituto de Cerámica y Vidrio (CSIC). Universidad Autónoma de Madrid, Spain, 2000.
23. Rincon, J. and Durán, A., Separación de fases en vidrios. El sistema Na_2O–B_2O_3–SiO_2. Monograf'ias de la Sociedad Española de Cerámica y Vidrio. Arganda de Rey (Madrid) 1982.
24. Völksch, G. and Heide, H., Dissolved gases and minor component effects on glass crystallization. *J. Non-Cryst. Solids*, 1977, **219**, 119–127.
25. Scherer, G. W., Sintering of low-density glasses; I, theory. *J. Am. Ceram. Soc.*, 1977, **60**, 236–239.
26. Brinker, C. J. and Scherer, G. W. Sintering. In *The Physics and Chemistry of Sol-Gel Processing* Chapter 11. Academic Press, 1990, pp. 675–747.
27. Bordia, R. K. and Raj, R., Role of shear in the sintering of

composites. In *Tailoring Multiphase and Composites Ceramics*, ed. R. E. Tressler, G. L. Messing, C. G. Pantano and R. E. Newnham. Plenum, New York, 1986, pp. 27–39.
28. Bordia, R. K. and Raj, R., Analysis of sintering of composite with a glass or ceramic matrix. *J. Am. Ceram. Soc.*, 1986, **69**, C–55-C-57.
29. Ducamp, V. C. and Raj, R., Shear and densification of glass powder compacts. *J. Am. Ceram. Soc.*, 1989, **72**, 798–804.
30. Sura, V. M. and Panda, P. C., Viscosity of porous glasses. *J. Am. Ceram. Soc.*, 1990, **73**, 2697–2701.
31. Boccaccini, A. R., Sintering of glass powder compacts containing rigid inclusions. *Science of Sintering*, 1991, **13**, 151–161.